NGR-36-027-068

MODERN OPTICS

CASE WESTERN RESERVE UNIVERSITY

UNIVERSITY CIRCLE • CLEVELAND, OHIO 44106

FAR INFRARED MASER COMMUNICATIONS TECHNOLOGY

Final Report

NASA Grant NGR 36-027-068

FINAL REPORT

FAR INFRARED MASER COMMUNICATIONS TECHNOLOGY

Period Covered: May 13, 1974 to November 30, 1975

NASA Grant NGR 36-027-068

Principal Investigators

Paul C. Claspy
Yoh-Han Pao

Department of Electrical Engineering and Applied Physics
Case Western Reserve University
Cleveland, Ohio 44106

NASA Technical Officer

Nelson McAvoy

NASA Goddard Space Flight Center

Greenbelt, Md.

TABLE OF CONTENTS

FAR INFRARED MASER COMMUNICATIONS TECHNOLOGY

1. Preface

This document reports on the activities and principal results of a program on far infrared maser communications technology carried on at Case Western Reserve University, supported by NASA Grant No. NGR 36-027-068.

2. Summary of Principal Results

a. An optically pumped FIR laser has been constructed and tested. Optimum operating conditions have been determined with CH_3OH as the lasing medium. The laser has been found to operate equally well with flowing gas or in a sealed off configuration. We have found that FIR cavity stability and pump laser stability are significant problems and steps are being taken to correct this.

b. We have measured the absorption coefficient per unit pressure of 1-1 difluoroethylene at the P(22) and P(24) lines of the 10.4 micron CO_2 band. The FIR line pumped by P(22) occurs at ~890 microns, which may be in an atmospheric transmission window.

c. We have found that significant Stark tuning of absorption lines of methanol and 1-1 difluoroethylene can be accomplished, even at the usual 100 to 300 mTorr operating pressures of FIR lasers. This means that the use of Stark tuning may enable more effective use of pump laser output.

3. Far Infrared Laser Studies

a. Introduction. The far infrared (FIR) or submillimeter portion of the electromagnetic spectrum was of considerable interest in the 1950's because of the need for additional carrier frequencies for communication systems. After a significant number of fundamental investigations, however, further work was delayed until efficient, long-lived sources of such radiation became available.

Although direct excitation electric discharge FIR lasers, such as the HCN laser, have been known for many years, further interest in the application of FIR wavelengths to communications systems was not aroused until the report of the first optically pumped FIR laser by T. Y. Chang in 1970.

So far, the approach which has worked the best consists of pumping a molecular gas with a CO_2 laser. By selecting the appropriate CO_2 transitions, a large number of gases may be made to exhibit gain in the FIR wavelength region. Although one depends in general on an overlap between the CO_2 pumping wavelength and the molecular gas absorption, there is indication that off-resonance pumping is also feasible and in general Stark field tuning may be used to improve the overlap.

Several synthetic polymeric materials and inorganic materials such as CdTe and GaAs are sufficiently transparent in the FIR wavelength region to serve as windows and/or mirror substrates. Thermistors are suitable for detecting slowly varying signals and silicon point contact diode structures may be used for high frequency signals.

In general, enough is known to suggest that FIR masers are potentially useful devices especially for communications because of the high antenna gain available in structures of reasonable size and the opening up of a new spectral region to alleviate the crowding at lower frequencies. The main difficulty in establishing the future role of the submillimeter, or FIR, region is that data specific to the development of a viable communications technology in this frequency region is sorely lacking. Current data merely establishes the existance of laser lines, their output powers and pumping efficiencies, but little else.

An optically pumped FIR laser has been constructed and preliminary measurements have been made. A description of the device, along with the results obtained to date are given below.

b. System Description. The FIR laser is pumped by a flowing gas CO_2 laser tuned to P(36) of the 9.4μ band. The discharge tube is Pyrex, 70 cm long, 10 mm I.D. containing two discharge sections formed by two Nickel cathodes and a single tungsten pin anode and terminated at each end by ZnSe brewster-angle windows. Operating pressure is typically 21.5 Torr at discharge currents of 18 mA/section. The current in each discharge section is maintained at a constant value by high-voltage current regulators. The optical resonator is formed by a 2 meter radius of curvature 80% reflection germanium output mirror and an aluminum-coated copper grating of 150 lines/mm operated in Littrow (PTR Optics ML-303). The optics are supported by stainless steel mounts, Burleigh SG-201, bolted to aluminum end plates. The

length of the cavity is passively stabilized by connecting the optics mounts with three 1-inch diameter Invar rods. The discharge tube is supported from the Invar rods by micarta supports. The output mirror is mounted in a Model ED-25 Piezoelectric crystal stack manufactured by Jodon Engineering. The laser may be actively stabilized using a Lansing-lock-in stabilizer (Model 80.214) which modulates one section of the piezoelectric crystal stack at 520 Hz and detects the resulting amplitude modulation in the zero-order output from the grating using a Harshaw PY-4 pyroelectric detector. This laser is capable of producing 12 watts at band center and can be tuned to approximately 70 transitions in the 9.2-10.8 micron region. At P(36) of the 9.4μ band the output power is 4 watts TEM_{00} and 7 watts in higher order transverse modes. Diagram of the system is shown in Fig. 1.

The output from the CO_2 pump laser is mechanically chopped at 13 Hz with a 50% duty factor and then focused into the FIR laser using a Coherent Radiation germanium lens of 13.5 cm effective focal length.

The FIR laser resonator is formed by a 70 cm long gold-plated brass guide tube of 12.5 mm ID terminated by plane (flat) aluminum mirrors at each end. Both mirrors were produced by a commercial lapping firm and were lapped flat to within .50μ . The RMS surface roughness is 4μ . The CO_2 pump radiation is focused into the cavity through a tapered 1.2 mm (3/64-inch) dia hole in the mirror center as shown in Fig. 2 . To the limits of our measuring equipment, a Coherent Radiation Model 201 Power Meter, approximately 100% of the pump power is coupled through the 1.2 mm dia hole

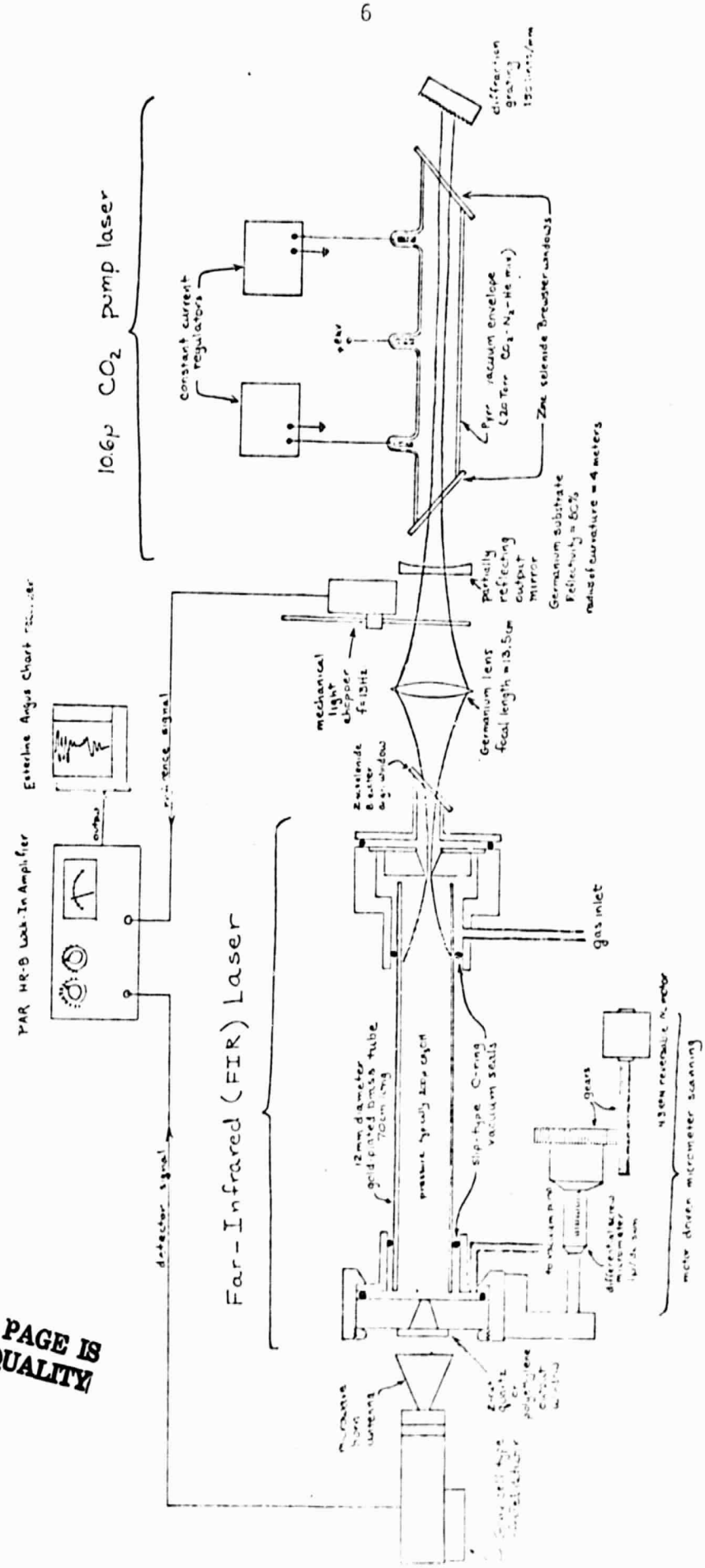

Figure 1. Schematic Diagram of Experiment

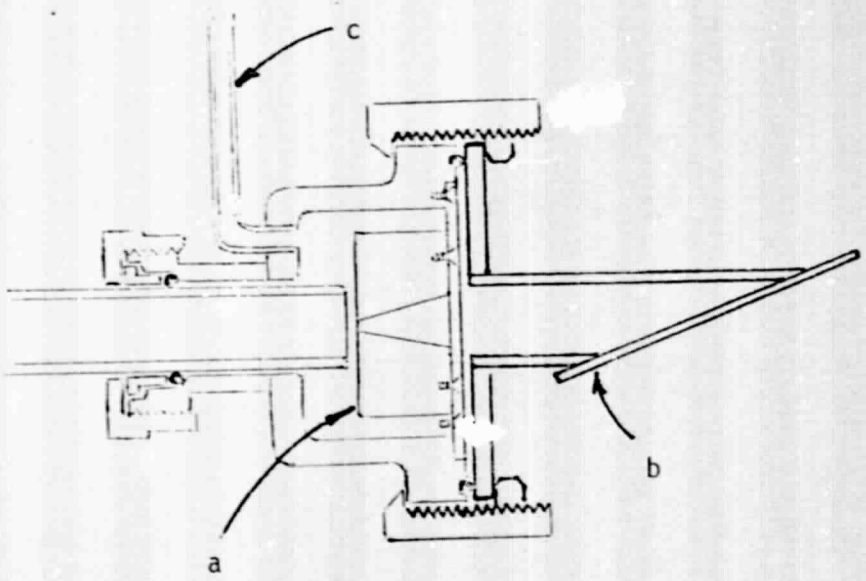

Figure 2. Pump Radiation Input End of FIR Laser

a. Mirror

b. ZnSe Brewster Window

c. Vacuum Line

even when the pump laser is operating in higher order transverse modes. The FIR laser vacuum is maintained by use of a Brewster angle ZnSe window to this input hole coupling mirror. The FIP output is taken through a 1.2 mm dia hole in the second mirror followed by an integral 32° radiation horn 1.2 cm long and terminated in a polyethylene window. The guide is within 3 mm of the mirror at each end. The output mirror assembly is mounted on a translational stage as shown in Fig. 3. This translation is permitted by using a CAJON O-Ring compression vacuum seal between the mirror assembly and the guide tube. The translational stage is a Lansing Model 20.505 with a 22.505 differential micrometer gear driven from a 4.3 RPM reversable motor. Figure 4 shows FIR laser.

All vacuum seals are either soldered or compression type O-ring seals. The methanol supply is a small vial of liquid mounted on the translating mirror assembly and connected to the laser through a Cajon fitting and a stainless steel bellows valve (see Fig. 5). The laser guide tube forms the vacuum envelope for the laser, there is no gas reservoir. The input mirror assembly is connected to a mechanical vacuum pump through a Hoke packed vacuum valve. Pressure is monitored at the input end by means of a CVC stainless steel Pirani gauge calibrated against a vacuum oil manometer and a calibrated (for air) Pirani gauge.

The FIR radiation is detected by a Harshaw PY-4 pyoelectric detector. A 1/8-inch thick piece of Teflon is used to filter out the CO_2 pump radiation passing through the polyethylene output window. On occasion a metal

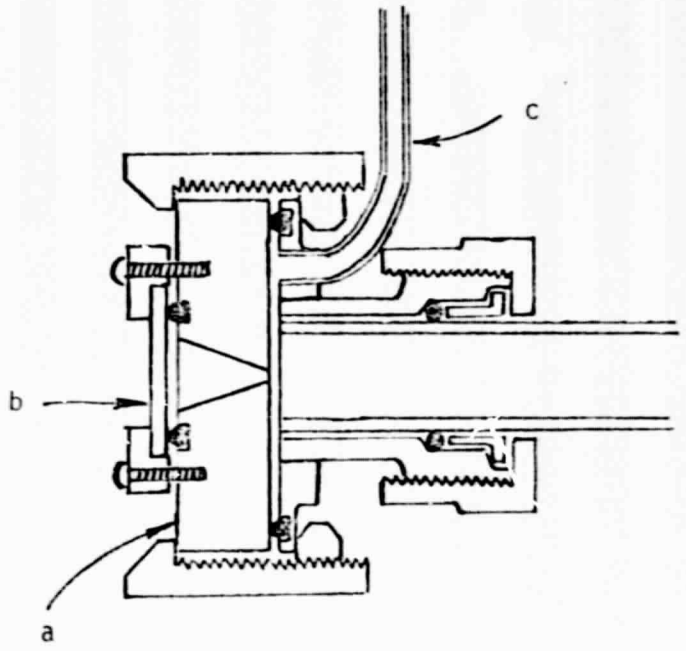

Figure 3. Far-Infrared Output End of FIR Laser

a. Mirror

b. Polyethylene or z-cut Quartz Output Window

c. Vacuum Line

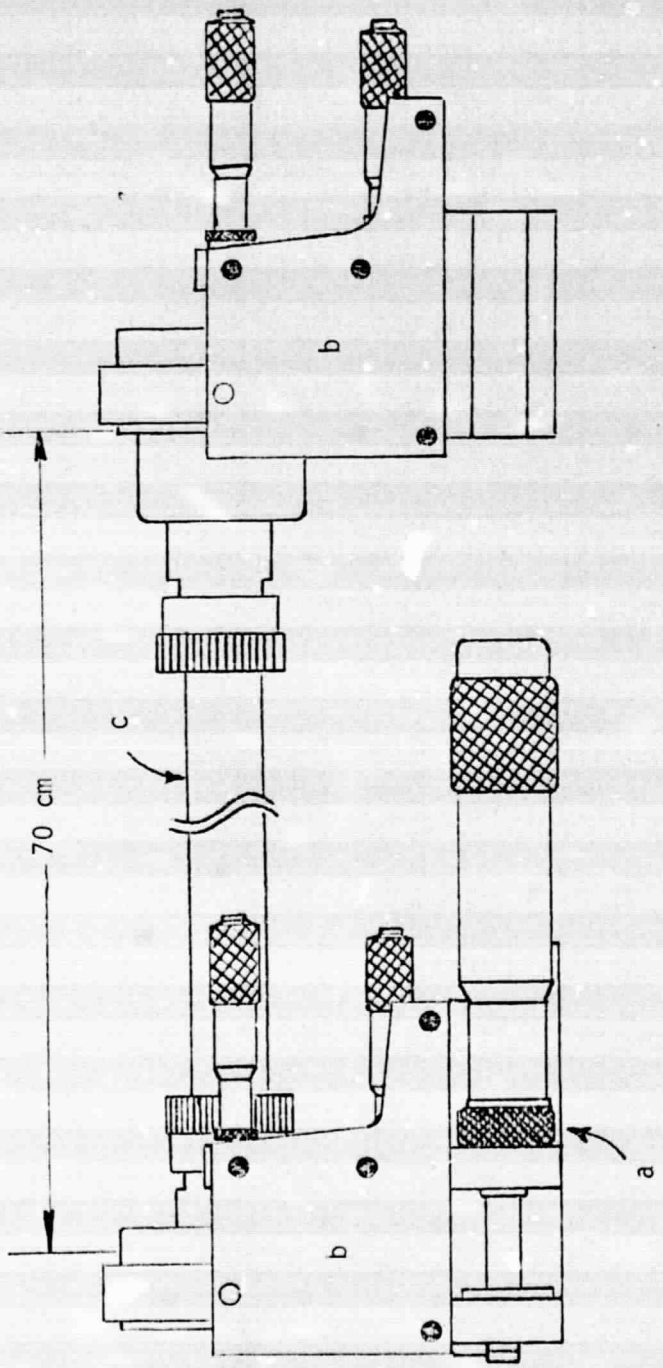

Figure 4. FIR Laser External Configuration

a. Translation Stage

b. Mirror Mount

c. FIR Laser Tube

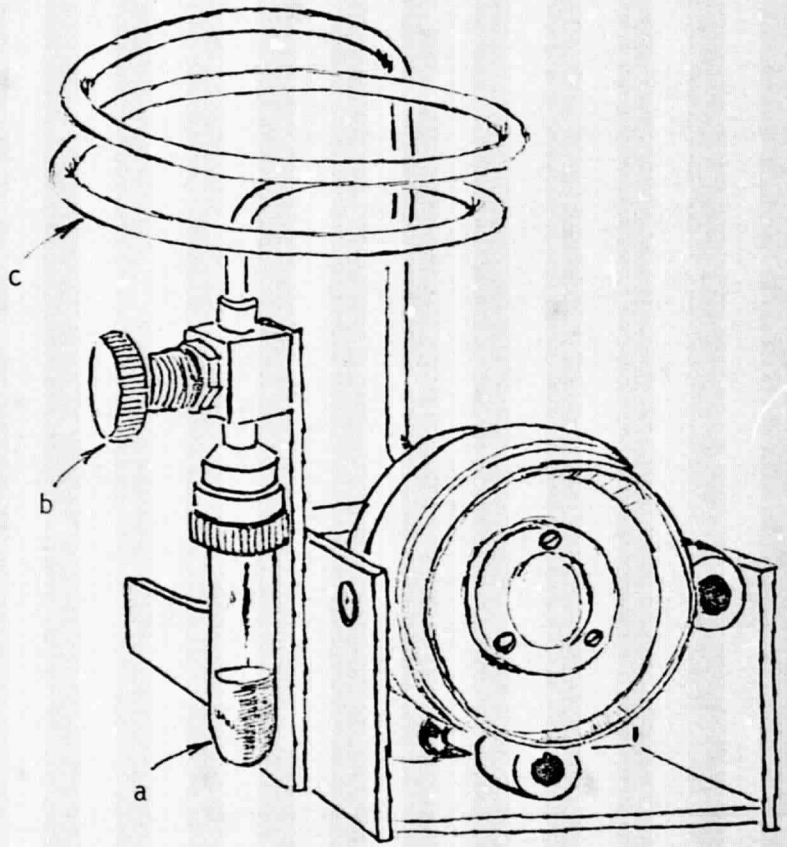

Figure 5. Diagram of Lasant Gas Supply System

a. Glass Vial of Methanol
b. CAJON Series "H" Stainless Steel Bellows Valve
c. Coiled Copper Tubing Allowing Alignment of Mirror

cone is used to collect the FIR output into the pyoelectric detector and increases the signal strength by a factor of two. No attempt has been made to focus the outnut onto the detector as yet. With the PY-4 pyroelectric detector's active area of 2 mm^2 , output signals in the range 1-10 millivolts have been measured using a Keithly 840 or PAR HR-8 lock-in amplifier.

c. Results. Optimum FIR laser pressure for 118 micron methanol operation is approximately 200 millitorr (see Fig. 6). At this pressure a large number of cavity modes is observed as the cavity length is scanned. Figure 7 shows a typical result of output power as a function of cavity length. As the pressure is increased to 300 millitorr most of the modes disappear leaving the two modes seen in Fig. 8 .

The amplitude of the laser output is not constant as seen by the slow variations in Fig. 7 . There are several factors which can lead to this type of amplitude variation, namely changes in the lasant gas pressure, mechanical instability in the FIR laser, and frequency instability in the pump laser. The effect of each of these factors can be considered separately.

When the FIR laser is operated with a slow flow of methanol the outlet gas pressure can be maintained to within 10 millitorr of the desired pressure, typically 100-200 millitorr, for periods of thirty minutes or more. In the sealed-off mode of operation the laser is filled with several torr of methanol and then pumped out to the desired operating pressure. The sealing-off of the laser is accompanied by a sharp rise in pressure, i.e.,

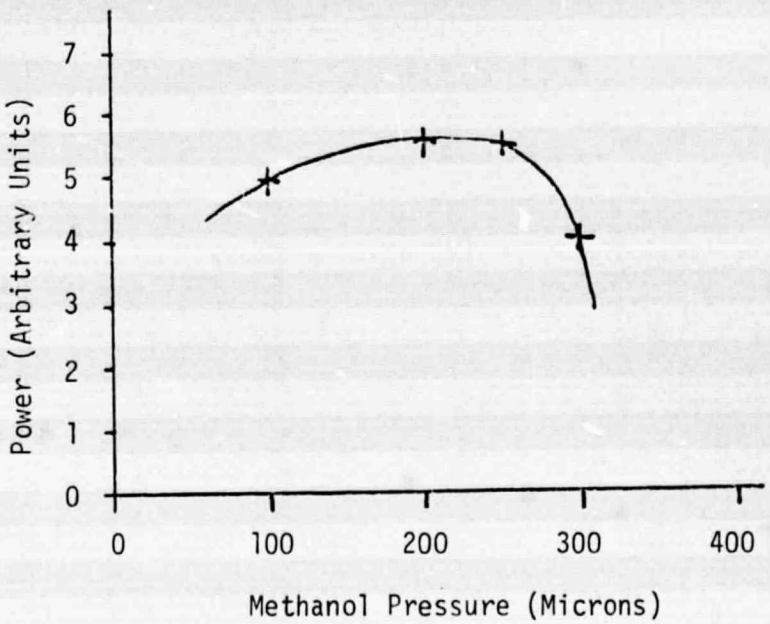

Figure 6. FIR Output Power as a Function of Methanol Pressure CW Pump Power = 5.0 watts 9.4μ P(36) pump laser frequency scanned

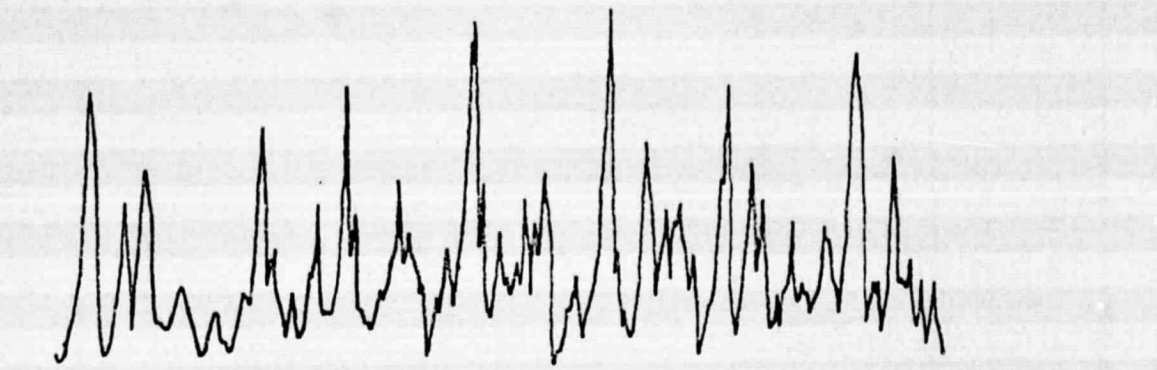

Figure 7. FIR Output Power as a Function of Cavity Length

Methanol Pressure = 200 millitorr (avg)

CW Pump Power = 5.1 w 9.4μ P(36)

Pump Laser Frequency Scanned

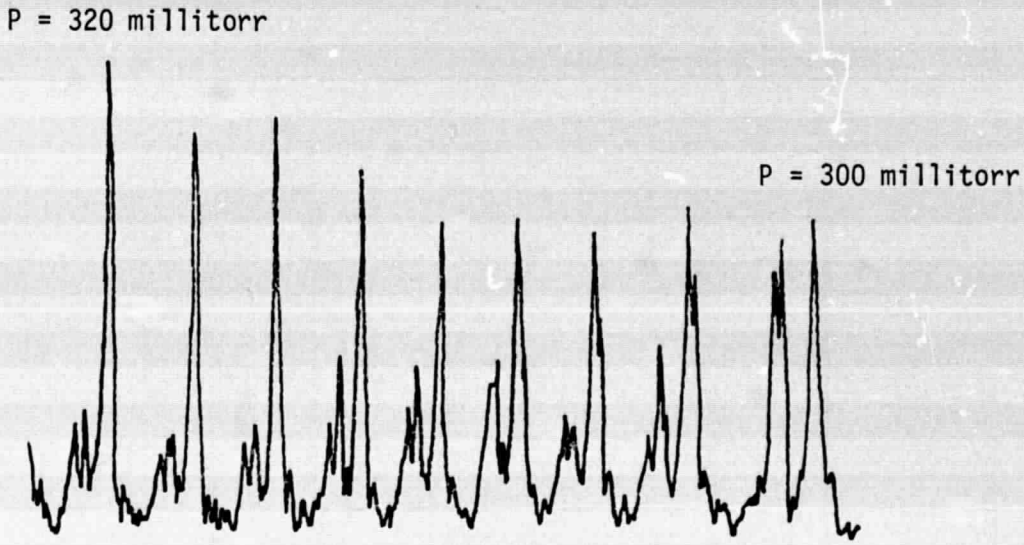

Figure 8. FIR Output Power as a Function of Cavity Length

Methanol Pressure = 310 millitorr (avg)

CW Pump Power = 5.0 watts 9.4μ P(36)

Pump Laser Frequency Scanned

several hundred millitorr in several minutes. Repeated pumping and sealing-off eventually stabilizes the gas pressure to within 10 millitorr of the desired pressure for a period of thirty minutes or longer. The cause of this pressure rise is assumed to be the evaporation of condensed methanol in the gas inlet line. This line is approximately twelve inches of 0.25-inch O.D. copper tubing formed into a double spiral. The purpose of this design is to permit limited motion between the gas supply bottle/valve assembly (which is bolted to a Lansing mirror mount on a translational stage) and the mirror assembly for alignment purposes. That methanol is indeed condensed in the inlet line was confirmed by heating the inlet line with a heat gun. The pressure in the laser immediately rose 100-200 millitorr and pumping on the laser while heating the inlet line permitted a stable gas pressure to be achieved with a single pumping operation. It is felt that gas pressure is not a major source of amplitude instability in the present experiments because of the relative stability of the pressure over a thirty minute period (the length of most experimental runs) and also because of the relative insensitivity of the FIR laser output to small excursions about the optimum gas pressure (see Fig. 6). It may be noted in passing that, although no experiments to actually measure the sealed-off lifetime of the laser were made, the laser can be routinely operated for two hour periods with no noticeable degradation of laser performance. On occasion the laser has been in operation for 6 to 8 hours without any refilling or pumping out of the laser.

The FIR laser was found to have considerable short-term mechanical instability associated with the translational stage/mirror assembly, i.e., if the laser length is tuned so that oscillation occurs, that laser line typically disappears within one minute. This is assumed to be due to relaxation of stresses on the sliding O-ring seal during translation. To isolate pump laser frequency instabilities from the mechanical instability of the FIR laser the pump laser frequency was mechanically varied (scanned) by applying a 5 Hz voltage ramp to the piezoelectric crystal stack. When a detection system time constant of 1-3 seconds is used, the detected FIR laser output is an average over the possible pump laser frequencies, thus eliminating any frequency instability inherent in the pump laser. The source of instability was further isolated by scanning the FIR laser cavity. The power of the 118 micron laser transition did not change appreciably over one complete scan of the laser cavity (1000 microns in 30 minutes) with the pump laser frequency mechanically scanned as explained above (see Fig. 7). A slow variation of laser amplitude can be seen in Fig. 7 but these variations are probably due to the much slower gas pressure variations rather than mechanical instabilities. When the pump laser frequency was mechanically scanned, the FIR cavity could be tuned to a desired laser line only after much patient readjustment of the FIR cavity length. Once adjusted in such a manner, the FIR laser was reasonably stable; in fact, on one occasion the cavity maintained the length setting overnight so that the laser still lased when turned on the following morning.

The pump laser frequency was also a source of instability in these experiments. For most experiments the pump laser frequency was mechanically scanned as previously mentioned to average out any instability in laser frequency. It was possible to operate the FIR laser at a fixed frequency corresponding to a maximum in FIR laser output only after considerable readjustment of the piezoelectric crystal stack voltage on the pump laser. This is probably due to thermal variations in cavity length and dimensional changes in the optics due to heating. Measurements of the stability of the pump laser were performed only after the FIR laser length remained stable for at least 20 minutes. It was found possible after considerable readjustment of the piezoelectric crystal stack voltage to operate the laser on a FIR line for a period of several minutes with ten minutes being the maximum achieved.

The major conclusions that can be drawn from this set of experiments are that the mechanical construction and stability of the FIR and pump lasers are inadequate for further research. The instability of the pump laser has been discussed, as has the mechanical relaxation problem encountered with the FIR cavity. The gas system did not appear to be a major problem although its effects were overshadowed by the mechanical problems. A major problem of the described FIR laser is that it proved impossible to change the operating pressure of the FIR laser, i.e., to operate the vacuum valves attached to the FIR laser, without affecting the cavity length. This is due to the mirror mounts being the major structural support for the laser.

An improved design would minimize mechanical coupling to the FIR laser mirror mounts for more operating stability. It should also eliminate the sliding O-ring seals to remove the mechanical relaxation problem.

4. Absorption and Stark Effect Studies

a. Introduction. The use of a particular molecular gas as a low threshold optically pumped FIR laser medium relies heavily on the overlap of a feature of its absorption spectrum with the emission spectrum of a suitable infrared pump laser. Furthermore, since the infrared absorption spectra of molecular gases at low pressure typically have a "picket fence" nature, and the output spectrum of the CO_2 laser, the usual pump source, also resembles a picket fence, coincidences between the two spectra can in a sense be regarded as "spectroscopic accidents". Many such accidents do occur, as evidenced by the number of optically pumped laser transitions which have been reported in the literature, although rarely is the optimum pump frequency coincident with the pump line center. Two questions come to mind, then, when considering the design of an optically pumped FIR laser, namely, what is the absorption coefficient of the FIR laser gas over the tuning range of the CO_2 pump transition, and can the optimum pump frequency be changed by Stark tuning the absorption spectrum. Some aspects of each of these questions have been investigated during the period of this grant.

b. System Description. A schematic diagram of the apparatus which was used both for absorption coefficient measurements and for Stark effect studies is shown in Fig. 9 . A water cooled 2 mm bore pyrex waveguide CO_2 laser was used as a probing source. The laser cavity consists of a 150 lines per mm, 92% blaze efficiency original diffraction grating and a flat 98% reflecting Ge output mirror. This laser has a maximum output power of

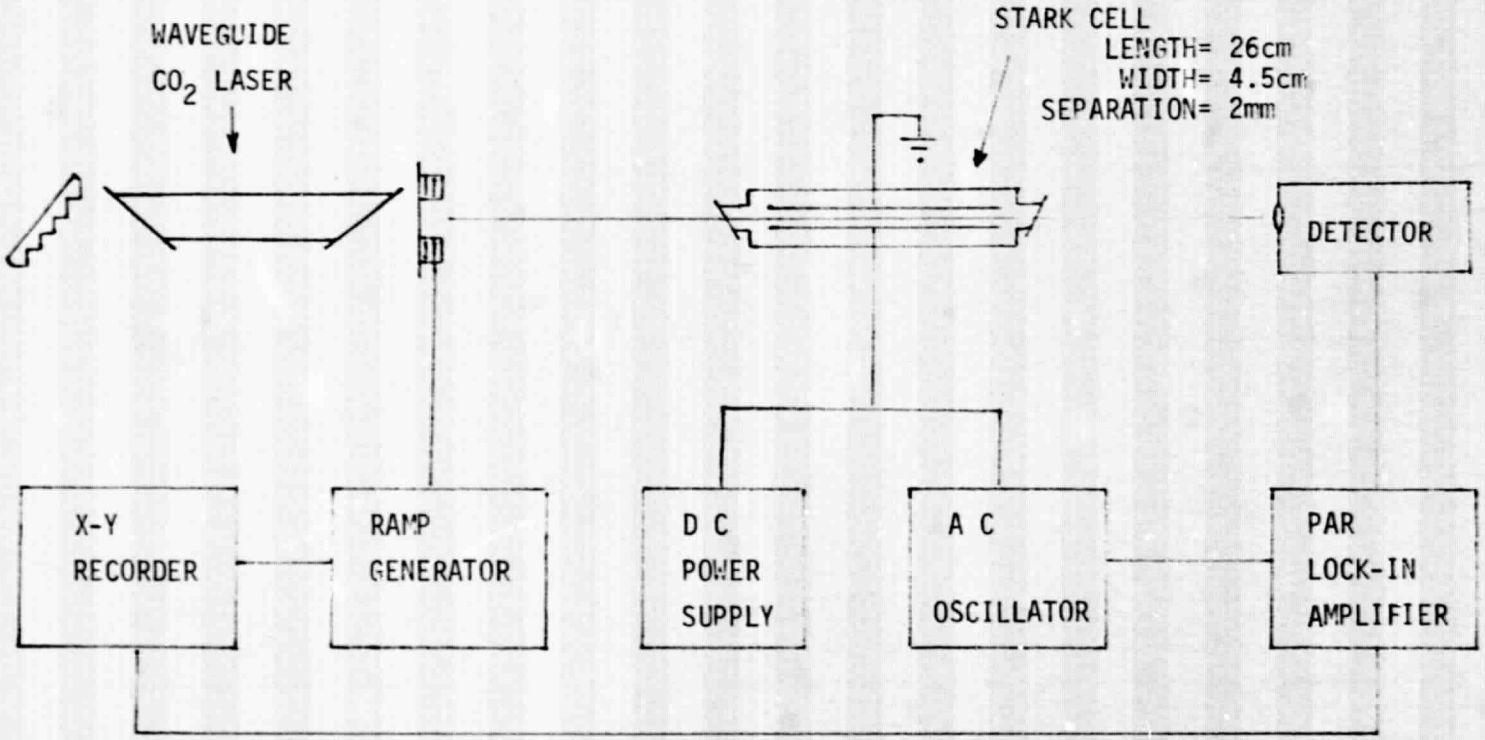

Fig. 9 Experimental Arrangements For Absorption And Stark Effect Studies

about 100 mw in the 10.4 micron band and about 40 mw in the 9.4 micron band. Although greater output powers can be obtained with higher coupling, this was purposely kept low to increase the laser tuning range. The results of a previous heterodyne study showed that with this cavity the laser has a tuning range of 230 MHz on the P(22) line of the 10.4 micron band when operated at an average (flowing) pressure of 45 Torr. The short term frequency stability is less than 4 MHz.

Two absorption cells were used at various times during the measurements. The first cell consists of a pyrex vacuum envelope containing two stainless steel Stark plates 26 cm long, 4 cm wide, and separated by 2 mm. The plates were hand polished with abrasive paper and steel wool. The second cell is a 1 m long pyrex tube with no Stark plates. Both cells have NaCl Brewster windows and the Stark cell can be rotated so that the electric field is either parallel to or perpendicular to the polarization of the incident radiation.

The transmitted radiation was measured either with a Coherent Radiation Model 201 Power Meter or with a Santa Barbara Model Ge:Au detector.

c. Absorption Coefficient Measurements. Measurements have been made of the absorption coefficient of 1-1 difluoroethylene ($C_2H_2F_2$) within the tuning range of the P(22) and P(24) lines of the 10.4 micron band of the CO_2 laser. These were accomplished by recording the output of the Ge:Au detector, which was located at the output end of the absorption cell, as the laser frequency was scanned through its tuning range. The measurement

was first done with the absorption cell evacuated, then with various pressures of $C_2H_2F_2$, ranging from ∿ 100 mTorr to 1.4 Torr.

Figure 10 presents the results of the transmission measurements as a function of $C_2H_2F_2$ pressures and frequency offsets from the laser line-center. The plotted transmissions are normalized to the laser gain curve. It can be seen that the absorption is nearly uniform over a laser frequency offset range of ± 60 MHz from line center. Figure 11 shows an oscilloscope display of the laser lineshape change due to absorptions by $C_2H_2F_2$ (the transmission observed here is not normalized). For comparison a similar study on the same gas at the P(24) CO_2 line is presented in Fig. 12. It shows that the absorption of $C_2H_2F_2$ gas at the P(24) line is peaked at about 50 MHz below the laser line center. From data presented in Fig. 10 we can obtain the total absorption of $C_2H_2F_2$ at the P(22) line for a 1M long absorption cell as a function of pressures at different frequencies as shown in Figs. 13, 14, and 15.

As a result of the absorption study, it can be seen that the $C_2H_2F_2$ in a 1M long $C_2H_2F_2$ FIR laser at a pressure of 200 mTorr will absorb only ∿ 15% of the pump laser power. To increase the total absorption, say to 90% of the pump laser power the pump laser beam should be reflected at least 6 times through the FIR cavity.

The laser peak power density throughout the absorption study experiment is about 300 mwatt/cm^2 , which is too low to permit a study of the saturation parameter without resorting to very low absorption pressures

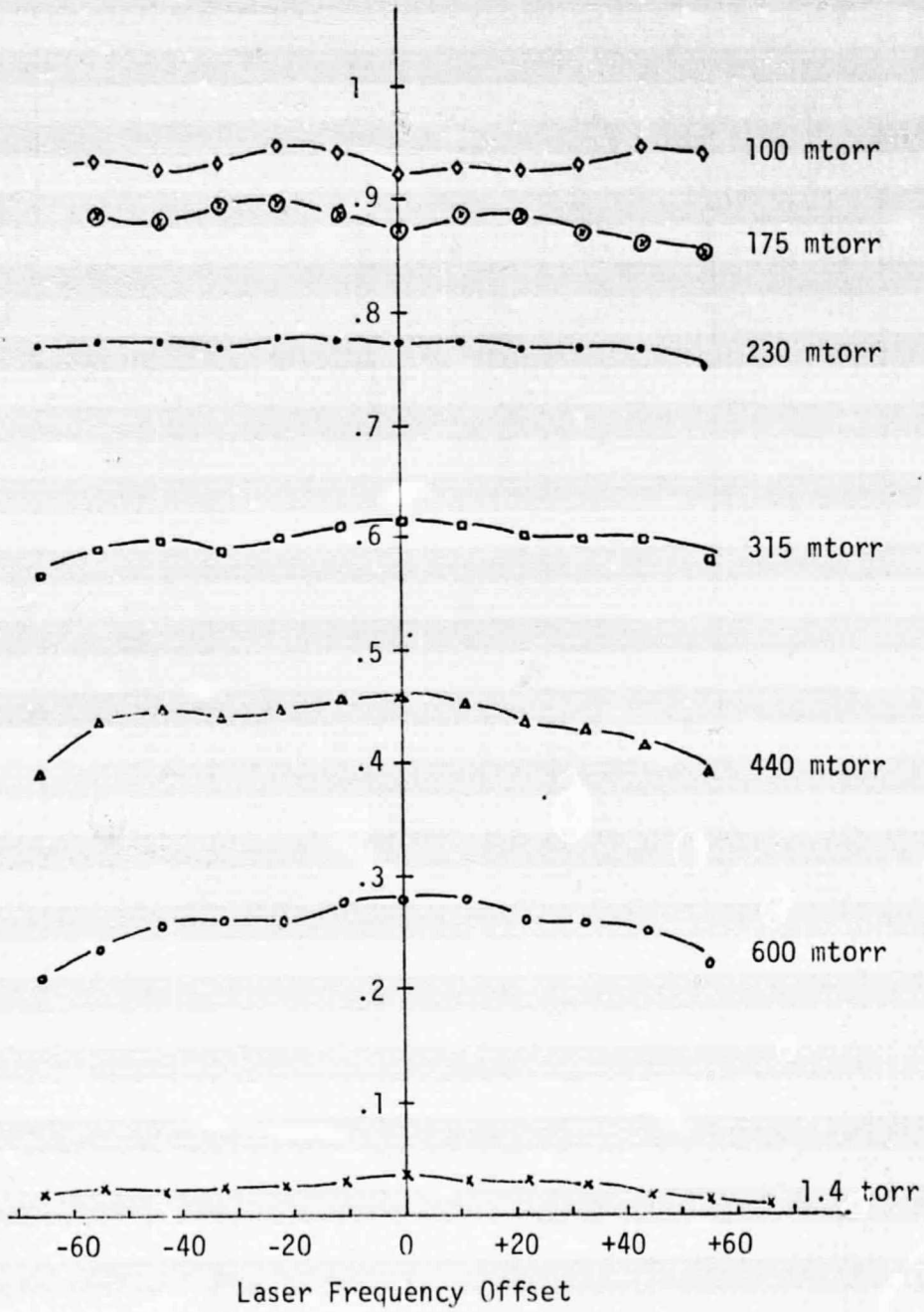

Figure 10. Normalized Transmissions for a 1 m Long Absorption Cell Filled with $C_2H_2F_2$ at Different Pressures as a Function of Frequency Offset from Line Center of P(22) of the 10.4 Micron CO_2 Band

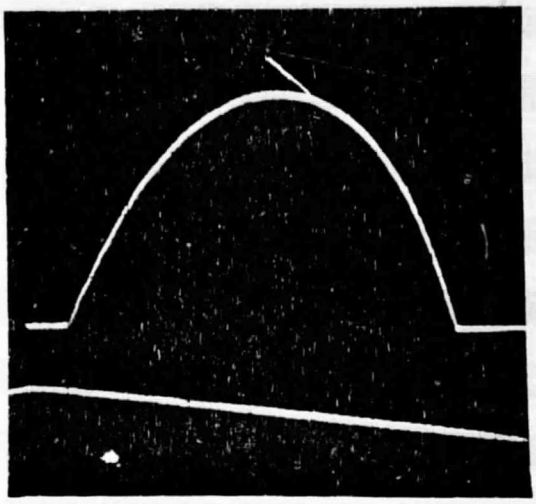

(a)

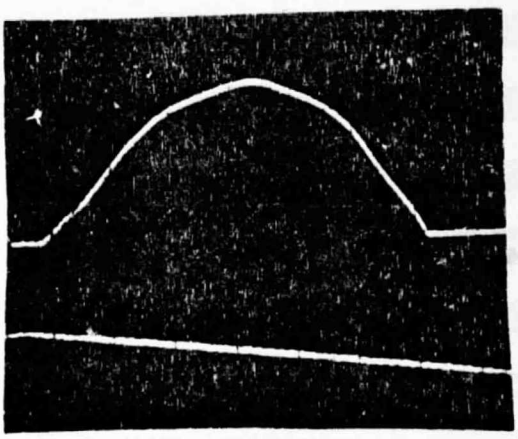

(b)

Figure 11. (a) P(22) 10.4 μm CO_2 Laser Tuning Curve, (b) Tuning Curve Change Due to 720 mtorr of $C_2H_2F_2$ in a 26 cm Long Absorption Cell. (The vertical and horizontal scales are the same in both photographs.)

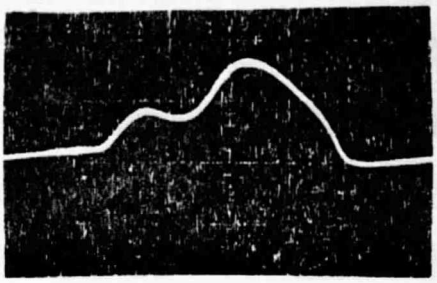

Figure 12a. P(24) 10.4 μm CO_2 Laser Tuning Curve as Modified by 720 mtorr of $C_2H_2F_2$ in a 26 cm Long Absorption Cell. (The unmodified curve was same as Fig. 11(a))

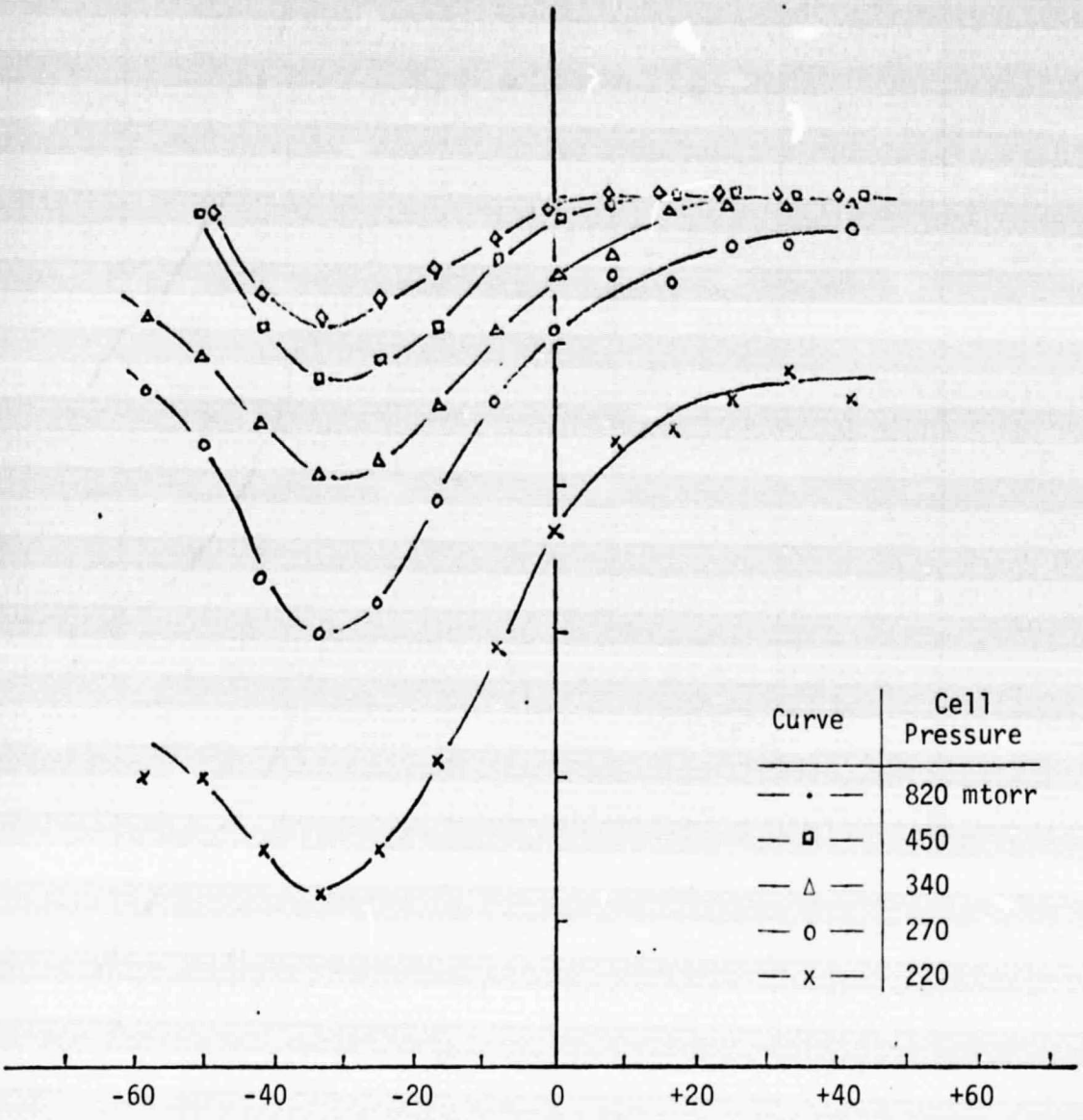

Figure 12b. Normalized Transmissions for a 26 cm Long Absorption Cell Filled with $C_2H_2F_2$ at Different Pressures as a Function of Frequency Offset from Line Center of P(24) of the 10.4 Micron CO_2 Band

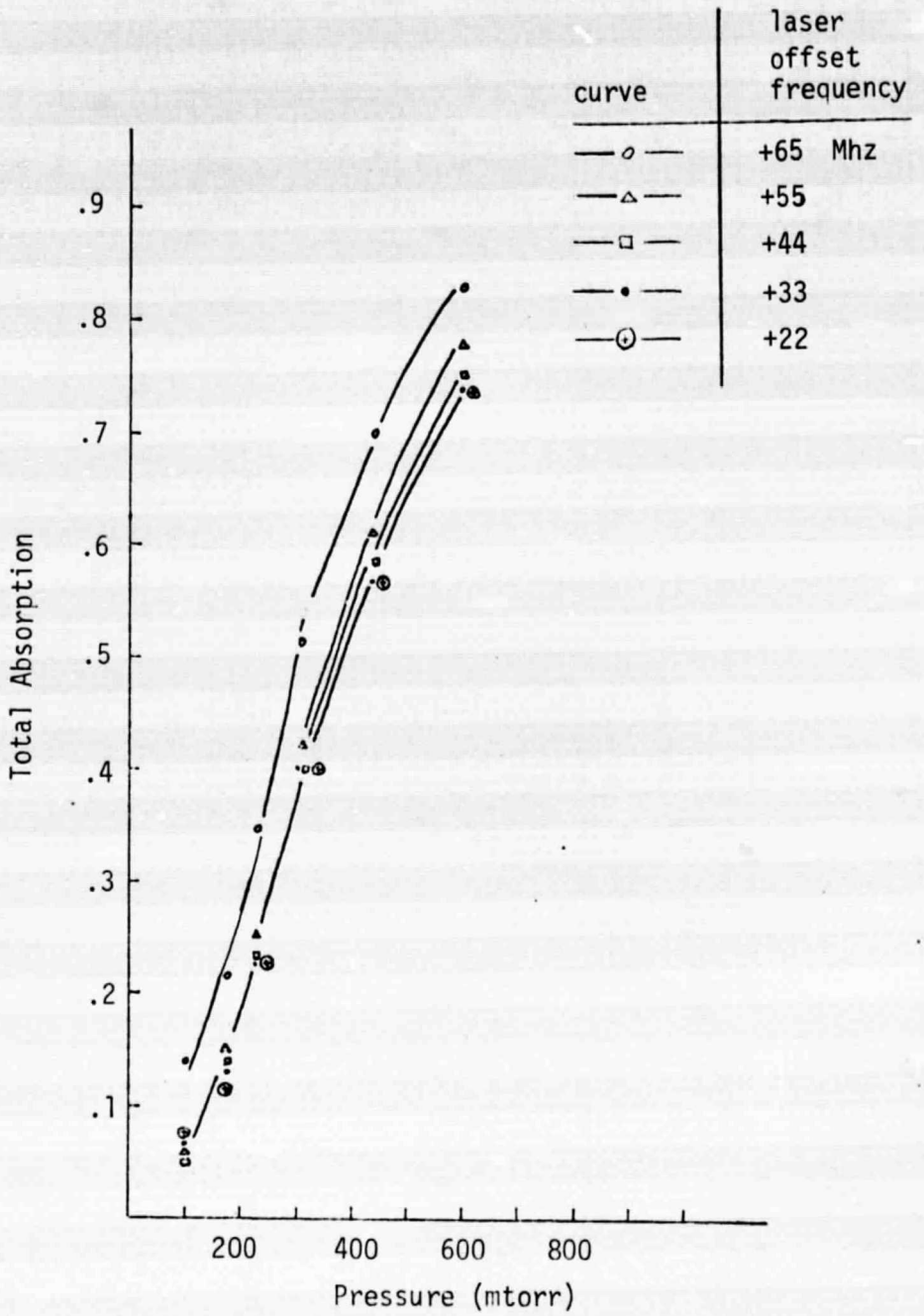

Figure 13. Total Absorption by $C_2H_2F_2$ Gas in a 1 m Long Absorption Cell at Different Pressures and Frequency Offsets from P(22) 10μ CO_2 Laser Line Center

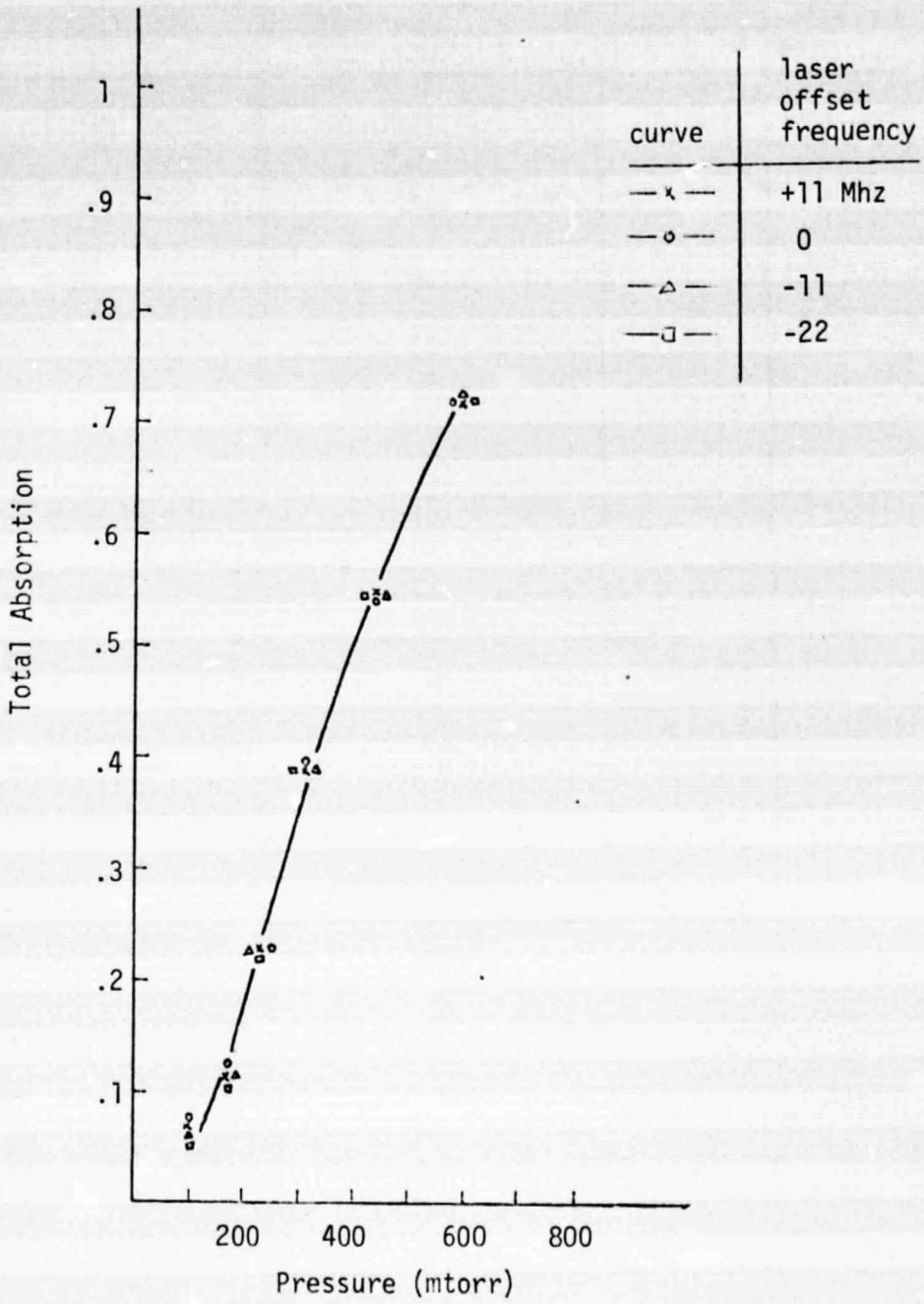

Figure 14. Total Absorption by $C_2H_2F_2$ Gas in a 1 m Long Absorption Cell at Different Pressures and Frequency Offsets from P(22) 10μ CO_2 Laser Line Center

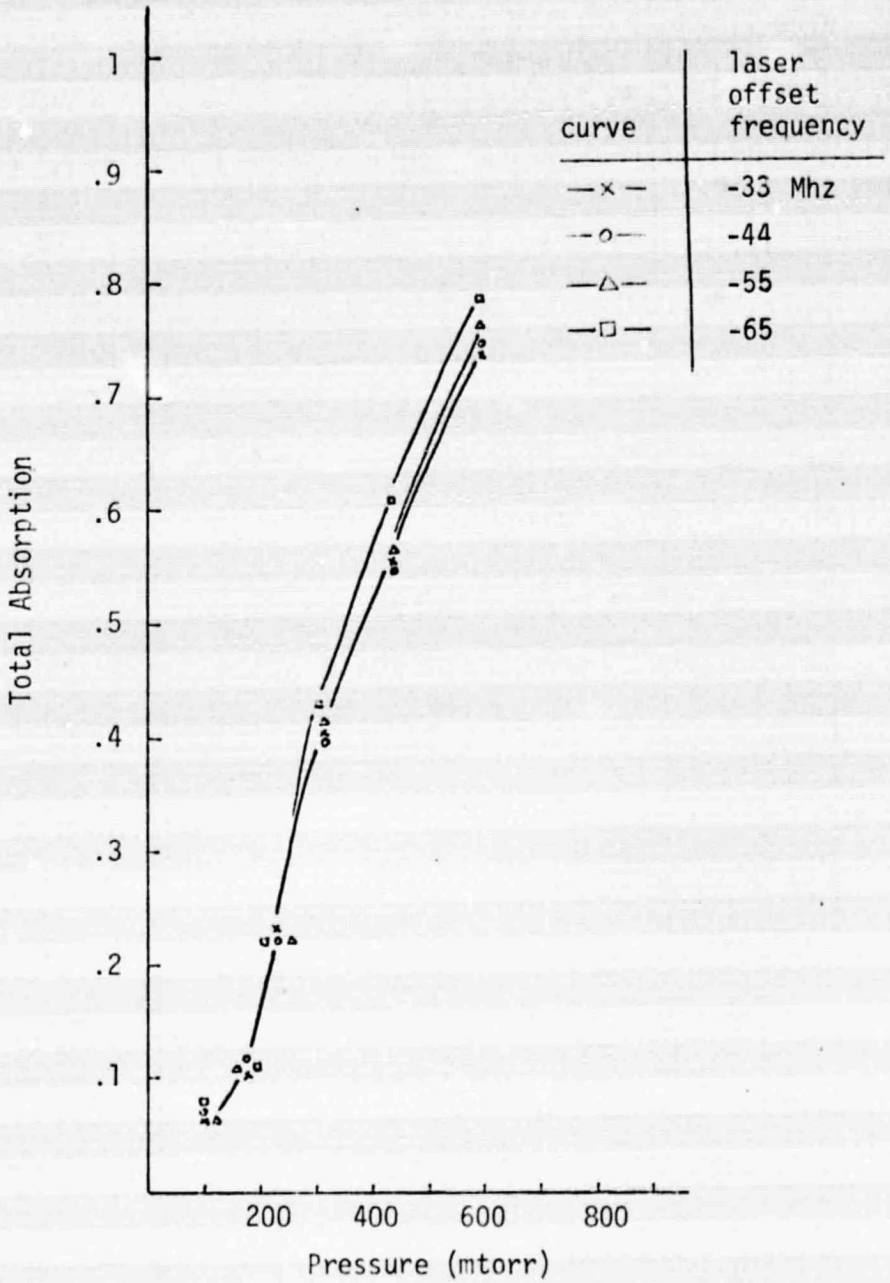

Figure 15. Total Absorption by $C_2H_2F_2$ Gas in a 1 m Long Absorption Cell at Different Pressures and Frequency Offsets from P(22) 10μ CO_2 Laser Line Center

or variable absorption cell length. As an alternative, a higher power density CO_2 laser is now being set up for studying the saturation parameter.

d. Stark Spectroscopy. The Stark spectroscopy studies which have been conducted during this investigation differ from the usual studies of this type in that they were all conducted at the pressures which are normally found in an optically pumped FIR laser. Thus we typically operated at pressures of 100 mTorr or higher rather than at 1 mTorr or less. While this higher than usual gas pressure results in lower maximum electric fields before gas breakdown occurs, because of the Paschen curve effect, it was felt that any practical FIR laser system must operate in this pressure range in order to achieve reasonable pumping efficiency. The objective of the study was to determine whether or not significant absorption tuning can be obtained at normal FIR laser operating pressures. Investigations have been made with methanol and 1-1 difluoroethylene, which are discussed separately below.

A search from P(10) to P(28) and R(10) to R(24) in the 9.4 micron CO_2 band indicates that CH_3OH gas has a number of significant absorptions within these laser lines. In particular, the CH_3OH absorption at P(12) of this band exhibits significant increase in absorption when the CH_3OH gas is Stark tuned. Figure 16 presents oscilloscope displays: (a) of the laser tuning curve alone, (b) of the laser tuning curve with 540 mtorr of CH_3OH gas in the absorption cell and no applied field, and (c) of the laser tuning curve with 540 mtorr of CH_3OH gas in the absorption cell and a 2 kv/cm Stark field. A Comparison of

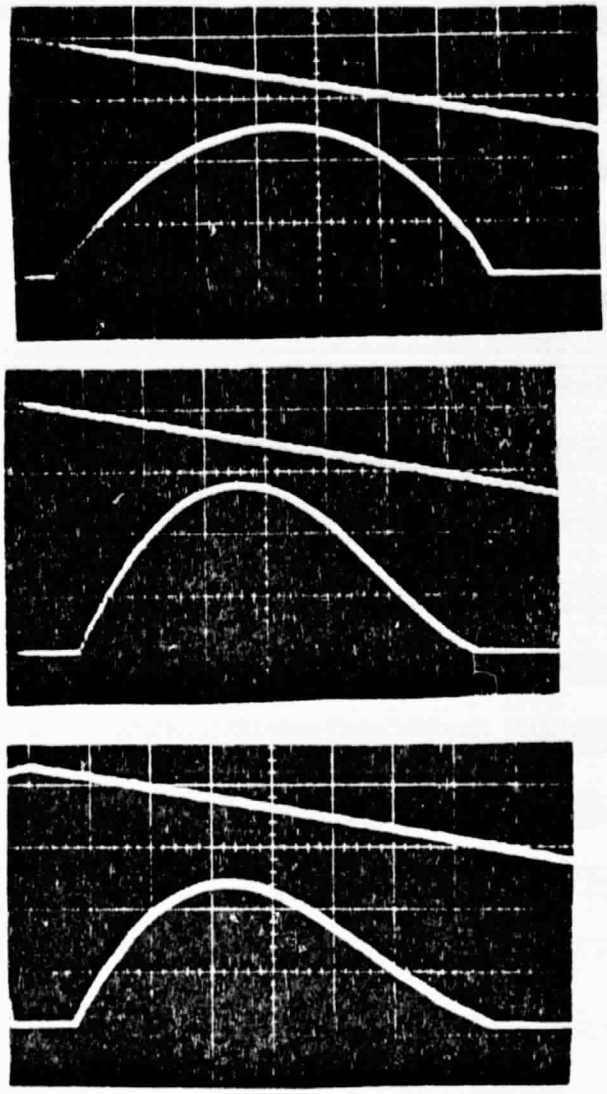

(a)

(b)

(c)

Figure 16. Changes in the P(12) 9.4 μm CO_2 Laser Tuning Curve Produced by Absorption of Methanol (CH_3OH). (a) Unattenuated laser tuning curve, vertical scale 0.2 V/cm; (b) laser tuning curve as modified by CH_3OH absorption (P = 540 mTorr, 26 cm absorber path length) with no external electric field, vertical scale = 0.1 V/cm; (c) same as (b) except with 2 KV/cm Stark field applied to CH_3OH .

Fig. 16b and 16c clearly shows an increase of absorption on the high frequency side of the laser tuning curve due to Stark tuning of the CH_3OH absorption. The continual increase in absorption with increase in Stark field is shown in Fig. 17, for three CH_3OH pressures--220 mTorr, 480 mTorr and 1.4 Torr. It can be seen that at CH_3OH pressures of 220 mTorr, 480 mTorr and 1.4 Torr, and when a Stark field of 2.3 kv/cm is used, the Stark-tuned absorption coefficients are 3.35×10^{-3} cm^{-1} , 7.0×10^{-3} cm^{-1} and 17.8×10^{-3} cm^{-1} respectively. The corresponding increases in absorption due to Stark tuning are 7%, 13% and 16 %.

The maximum Stark field that can be used in Stark-tuned absorption studies is determined by the CH_3OH gas breakdown in accordance with the Paschen relation for CH_3OH . The Paschen curve for CH_3OH has been determined by measuring the maximum allowable Stark field for various CH_3OH gas pressures without inducing gas breakdown. The results are shown in Fig. 18. The Paschen curve minimum of 2.25 kv/cm occurs at a pressure of 300 mTorr. As the pressure deviates from 300 mTorr higher Stark fields can be used.

A separate first derivative Stark spectroscopy study shows that a Stark field of 4 kv/cm appears to tune the line center of one of the Stark components to within the P(12) 9μ CO_2 laser tuning curve. This requires a CH_3OH gas pressure of 100 mTorr or below. At pressures above this the Stark spectrum appears to be unresolved and a general line broadening occurs.

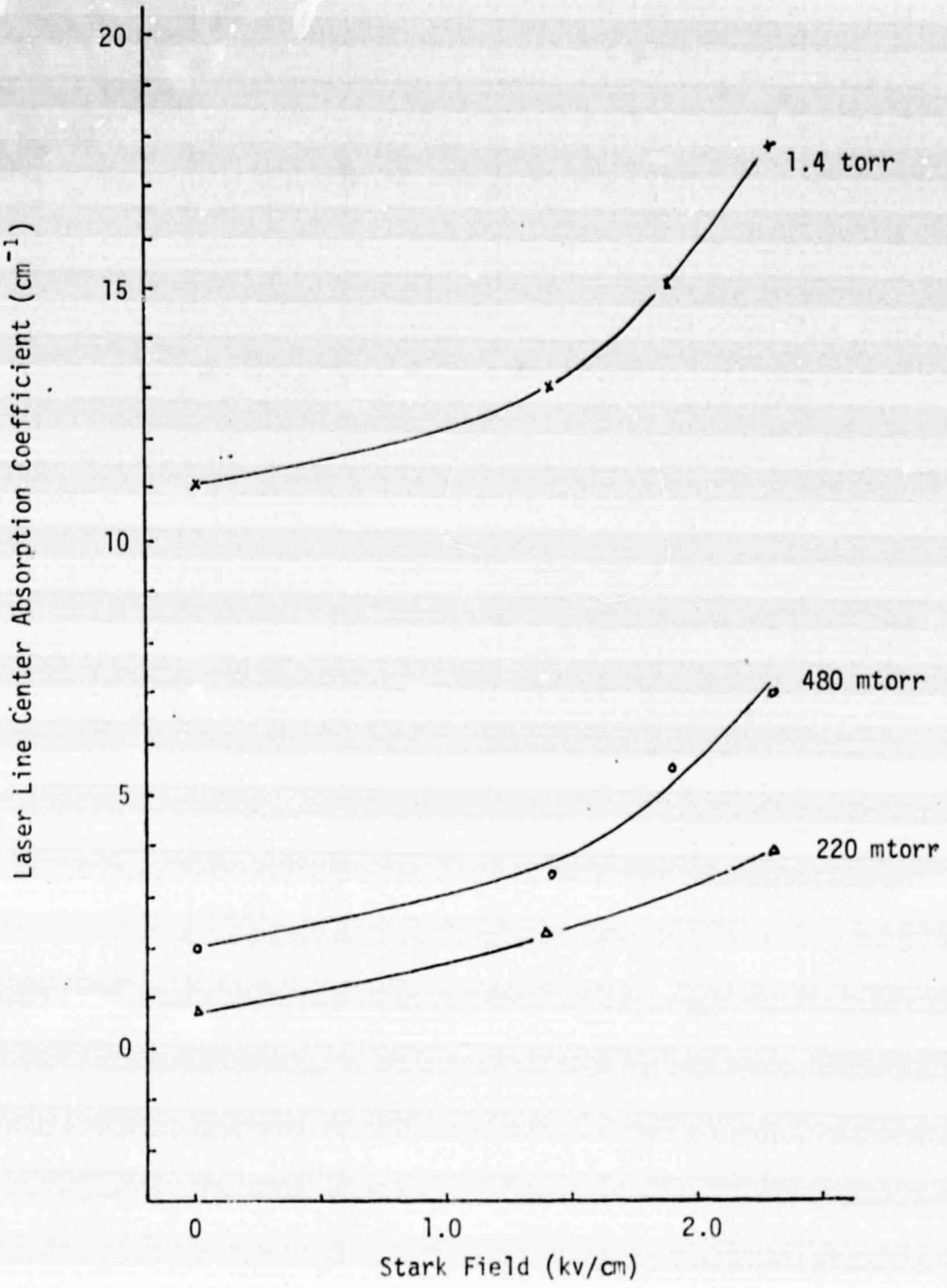

Figure 17. Absorption Coefficients of CH_3OH Vapor at the P(12) 9.4μ CO_2 Laser Line as a Function of Stark Field for 3 Different CH_3OH Pressures

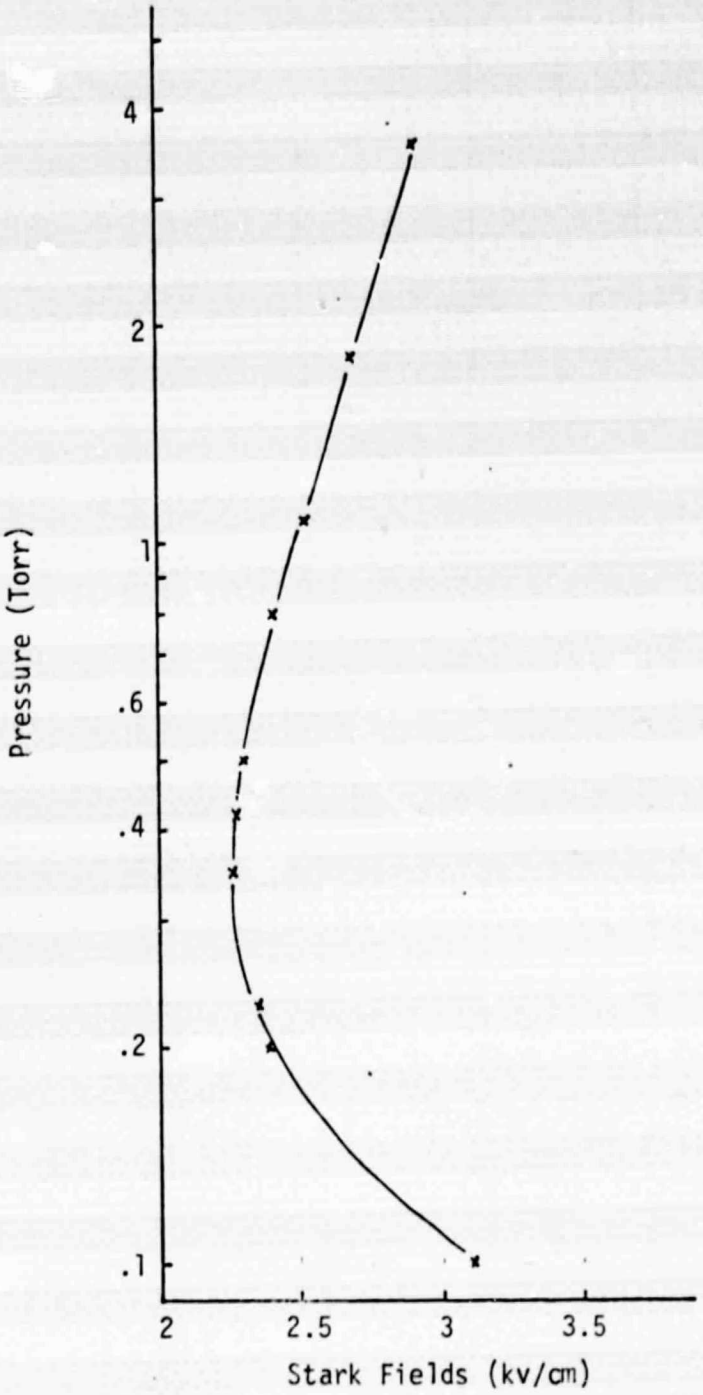

Figure 18. Maximum Stark Field as a Function of CH_3OH Pressure

The Stark behaviour of $C_2H_2F_2$ gas at the P(22) 10μ CO_2 line was investigated by a first derivative phase sensitive technique. This technique includes applying a small AC Stark field at a fixed frequency and a comparatively much larger DC Stark field on the Stark cell while the laser cavity is slowly scanned. The AC Stark field is to intensity modulate the laser beam and to provide an AC signal of the laser beam for phase sensitive detection. The DC Stark field is to Stark broaden or Stark shift the absorption components. Since the detected signal is the amount of laser modulation, which depends on the slope of the absorption profile, the detected signal is the first derivative of the absorption profile. This gives the derivative Stark spectroscopy a higher sensitivity in detecting narrow or weak absorption components.

The AC Stark voltage used range from 1 to 3 volts depending on the $C_2H_2F_2$ gas pressures. The DC Stark fields vary from 0 to 1.6 kv/cm. Figure 19 presents the Stark spectra of $C_2H_2F_2$ at P(22) of the 10.4 micron CO_2 band for a series of DC Stark fields. It can be observed that the absorption component is Stark broadened or shifted toward the high frequency side of the laser gain curve. At a Stark field of 750 v/cm, the absorption component starts to split up into two components. It has been noticed that the signal strength decreases with high Stark fields. This is expected because the absorption components are Stark broadened to cover a larger frequency span and part of it may even be outside the laser linewidth.

That a small Stark field of 50 v/cm on $C_2H_2F_2$ can produce a significant intensity modulation of a CO_2 laser beam, can be very favorable toward Stark

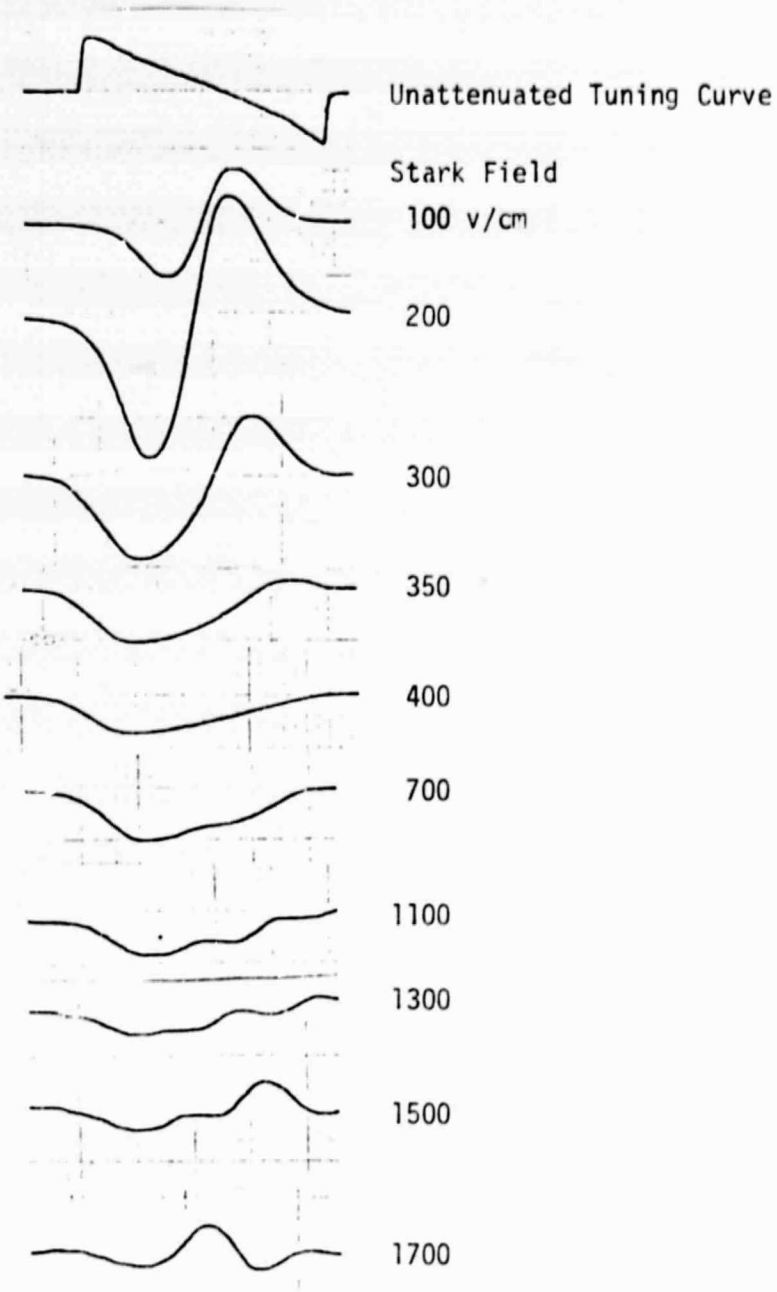

Figure 19. First Derivative Stark Spectra of $C_2H_2F_2$ at the P(22) 10.4μ CO_2 Laser Line as a Function of Stark Fields

modulating an optically pumped $C_2H_2F_2$ FIR laser. Also, that $C_2H_2F_2$ FIR gas shows Stark splitting of absorption component at Stark fields 750 v/cm, may introduce new FIR laser transitions. These and many other possibilities of Stark effect applications in an optically pumped FIR laser system are part of our plans for further investigations in FIR laser systems.